HHS Public Access

Author manuscript

ACS Nano. Author manuscript; available in PMC 2017 November 21.

Published in final edited form as:

ACS Nano. 2017 October 24; 11(10): 10135–10146. doi:10.1021/acsnano.7b04717.

Programmed Cell Death Protein Ligand-1 (PD-L1) Silencing with Polyethylenimine-Dermatan Sulfate Complex for Dual Inhibition of Melanoma Growth

Gijung Kwak[1,2], **Dongkyu Kim**[2], **Gi-hoon Nam**[1,2], **Sun Young Wang**[1,2], **In-San Kim**[1,2], **Sun Hwa Kim**[2], **Ick-Chan Kwon**[1,2], and **Yoon Yeo**[2,3,4,*]

[1]KU-KIST Graduate School of Converging Science and Technology, Korea University, 145 Anam-ro, Seongbuk-gu, Seoul 02841, Republic of Korea

[2]Center for Theragnosis, Biomedical Research Institute, Korea Institute of Science and Technology, Hwarangno 14-gil 5, Seongbuk-gu, Seoul 02792, Republic of Korea

[3]Department of Industrial and Physical Pharmacy, Purdue University, 575 Stadium Mall Drive, West Lafayette, IN 47907, USA

[4]Weldon School of Biomedical Engineering, Purdue University, West Lafayette, IN 47907, USA

Abstract

Programmed cell death protein-1 (PD-1) is a prominent immune checkpoint receptor interacting with its ligand, programmed cell death protein ligand-1 (PD-L1, B7-H1). The PD-1/PD-L1 interaction induces functional exhaustion of tumor-reactive cytotoxic T cells and, thus, interferes with antitumor T-cell immunity. In addition, PD-1/PD-L1 interaction promotes tumorigenesis *via* mTOR signaling pathway in a group of cancers including melanoma. Based on the dual functions of PD-1/PD-L1 interactions in tumor progression, we hypothesize that siRNA targeting PD-L1 (siPD-L1) will suppress melanoma growth, acting on both immune checkpoint and intrinsic tumorigenesis pathway. We tested this hypothesis by delivering siPD-L1 with a polymeric carrier ("pd") consisting of disulfide-crosslinked polyethyleneimine (CLPEI) and dermatan sulfate (DS), which we previously found to have a specific interaction with CD146- positive B16F10 melanoma cells. The siPD-L1/pd suppressed the expression of PD-L1 in the interferon-γ (IFN-γ)-challenged B16F10 melanoma cells in a cell-type dependent manner and attenuated the expression of tumor-specific genes in B16F10 cells. siPD-L1/pd suppressed the B16F10 melanoma growth in C57BL/6 immune-competent mice with increased tumor-specific immunity. siPD-L1/pd also suppressed melanoma growth in immune-compromised nude mice. Both animals showed a positive correlation between PD-L1 and p-S6k (a marker of mTOR pathway activation) expression in tumors. These results indicate that siPD-L1/pd complex attenuates melanoma growth in both T-cell dependent and independent mechanisms.

*Corresponding author: Yoon Yeo, Ph.D., Phone: 1.765.496.9608, Fax: 1.765.494.6545, yyeo@purdue.edu.

Supporting Information: Supporting Information is available free of charge *via* the Internet at http://pubs.acs.org. Supporting Information shows the effects of siRNA/pd complex on NIH 3T3 fibroblasts, the kinetics of PD-L1 expression in different cell lines, *in vitro* effects of PD-L1 silencing on melanoma-specific gene expression, *in vivo* results of low dose siPD-L1/pd complexes, and flow cytometry dot plots and histograms for immunophenotyping of tissues.

Keywords

siRNA delivery; polyelectrolyte carrier; immune checkpoint blockade; mTOR pathway; PD-L1; B16F10 melanoma

Programmed cell death protein-1 (PD-1) is a prominent immune checkpoint receptor on T cells, which interacts with its ligand PD-L1 to negatively regulate T cell function.[1] PD-1 is generally expressed on T cells and hematopoietic cells, and PD-L1 (B7-H1) is expressed on a wide range of non-hematopoietic cells including those in the tumor microenvironment.[2] PD-L1 is also expressed on cancer cells such as melanoma, non-small cell lung cancer, renal cell carcinoma, gastric cancer, leukemia, and multiple myeloma.[3] PD-1/PD-L1 interaction triggers functional exhaustion of tumor-reactive cytotoxic T cells, thus allowing tumors to evade antitumor immunity.[1,2] Blocking PD-1/PD-L1 interactions in tumors can reverse T cell exhaustion and induce significant anti-tumor responses[1] and has thus emerged as a promising strategy for cancer immunotherapy. Indeed, anti-PD-1 therapies such as pembrolizumab and nivolumab have shown impressive antitumor responses in clinical trials[4–7] and gained accelerated approval from the US FDA for the treatment of ipilimumab-refractory melanoma.[8]

In addition to the role in the immune checkpoint, recent studies uncover direct involvement of PD-1/PD-L1 signaling in tumorigenesis. Malignant melanoma contains PD-1 expressing cell subpopulations, which interact with host- and tumor PD-L1 to activate effectors of mTOR signaling pathway and promote tumor growth.[9] A recent study also shows that tumor-expressed PD-L1 promotes the growth and metastatic spread of melanoma and ovarian cancer cells by regulating mTOR signaling and autophagy.[10] Accordingly, the blockade of PD-1 or PD-L1 inhibits tumor growth even in the absence of a functional adaptive immune system.[9, 10]

Based on the dual functions of PD-1/PD-L1 interactions in tumor progression, we hypothesize that siRNA targeting PD-1/PD-L1 interactions delivered to B16F10 tumors will effectively suppress melanoma growth. We choose to target PD-L1 due to its expression in broad cell populations in tumor microenvironment.[2] Although most clinically-used inhibitors of PD-L1 are based on monoclonal antibodies,[3] we use siRNA to suppress PD-L1 expression because of the high target-specificity,[11] the ability to limit de novo production of PD-L1,[12] and the potential to combine with siRNAs of different functionalities in a single delivery.[13] For the delivery of siRNA targeting PD-L1 (siPD-L1), we use a polymeric carrier consisting of disulfide-crosslinked polyethyleneimine (CLPEI), a polycation used for gene complexation, and dermatan sulfate (DS) that neutralizes the excessive cationic charge of CLPEI. The CLPEI/DS (dubbed “pd”) complex has specific toxicity to a group of cancer cells that express CD146, including B16F10 melanoma cells, which is an advantage compared to other polymeric gene carriers.[14]

In this study, we hypothesize that siPD-L1 delivered by the pd complex can suppress melanoma growth *via* multiple mechanisms, including the melanoma-specific toxicity of pd complex and intrinsic and extrinsic anti-tumor effects of PD-1/PD-L1 blockade. With B16F10 murine melanoma cells and tumor models in immune-competent and immune-

compromised mice, we demonstrate that siPDL1/pd reduces the expression of PD-L1 in tumors and attenuates tumor growth by promoting cytotoxic T-cell immunity and suppressing mTOR pathway.

RESULTS

Characterization of siRNA/pd complexes

CLPEI was synthesized by crosslinking LPEIs via dithiobis(succinimidyl propionate) (DSP),[15,16] which introduces disulfide bonds between LPEI's (1.18 disulfide bonds per two LPEIs).[15] The formation of CLPEI was previously confirmed by the reduction of the N/P ratio that formed a complex with nucleic acids[15] and the appearance of a broad peak in gel filtration chromatography (GFC) corresponding to the increased molecular weight relative to LPEI's.[16] Given that the GFC consists of multiple peaks,[16] it is likely that CLPEI is a mixture of disulfide-crosslinked and uncrosslinked LPEI's. siRNA/pd ternary complexes were formed by sequential incubation of siRNA with CLPEI ('p') and DS ('d') (Figure 1a). siRNA and CLPEI formed an electrostatic binary complex at a CLPEI/siRNA weight ratio of 1 or higher (Figure 1b) with an average diameter ranging 230–290 nm, as measured by dynamic light scattering (DLS) (Figure 1c). The binary complex showed increasing toxicity with the addition of CLPEI, likely due to the increasing cationic charge (Figure 1d). A binary complex with a CLPEI/siRNA ratio of 2 was used to make a ternary complex based on the small size. Ternary complexes were prepared varying the DS/CLPEI weight ratio. The particle size did not change significantly, but the cationic charge was neutralized with the addition of DS (Figure 1e). Ternary complexes prepared with a relatively small amount of DS (DS/CLPEI ratio of 0.3 or 1) showed reduced toxicity compared to the binary complex reflecting the charge neutralization. However, the ternary complex prepared with the DS/CLPEI ratio of 2 showed greater toxicity than the binary complex (Figure 1f), consistent with our earlier observation.[14] Since the toxicity of the ternary complex is specific to B16F10 cells and desirable for therapeutic purpose, a ternary complex with a weight ratio of siRNA:CLPEI:DS of 1:2:4 was chosen for this study. Transmission electron microscopy found siRNA/pd ternary complex to have a spherical shape with a diameter between 200–250 nm (Figure 1g and h), slightly smaller than the DLS measurement, likely due to dehydration of the particles during the sample preparation.

siPD-L1/pd complex silences PD-L1 expression in B16F10 melanoma cells

We previously showed that DS in pd complex helps B16F10 cells take up the complex *via* CD146, a transmembrane glycoprotein overexpressed in melanoma cells.[14] To confirm the melanoma-specific uptake, the complex containing Cy5-labeled siRNA was incubated with B16F10 melanoma and NIH 3T3 fibroblasts. Both fluorescence microscopy and flow cytometry supported that siRNA/pd interacted with B16F10 cells (Figure 2a, b) but not with NIH 3T3 cells (Figure S1a, b). In contrast, siRNA/Lipo (siRNA/Lipofectamine2000 complex) entered both cell lines with no cell specificity.

The gene silencing effect of siPD-L1/pd was tested with the two cell lines. In tumors, interferon-γ (IFN-γ) is produced by tumor-infiltrating cytotoxic T lymphocytes (CTLs) and induces the expression of PD-L1 on tumor cells.[17–19] To mimic this condition *in vitro*, the

cells were incubated with 25 ng/mL of IFN-γ. B16F10 cells responded quickly and expressed PD-L1 twice as much as those receiving no IFN-γ treatment, right after 4 h incubation with IFN-γ (Figure S2). NIH 3T3 also expressed PD-L1 in response to IFN-γ but more slowly than B16F10 cells, reaching the maximum in 12 h post-IFN-γ incubation (Figure S2). These cells were treated with PBS, siNeg/pd (pd complex containing siRNA irrelevant to PD-L1) and siPD-L1/pd after 4 h incubation with IFN-γ. Consistent with the B16F10-specific uptake of siRNA/pd, PD-L1 silencing occurred in B16F10 cells (Figure 2c, d) but not in NIH 3T3 cells (Figure S1c). In the IFN-γ-treated B16F10, siPD-L1/pd reduced the PD-L1 expression by 50.9 % and 47.6 % compared with PBS and siNeg/pd, respectively. On the other hand, neither siPD-L1/pd nor siNeg/pd suppressed PD-L1 expression in the IFN-γ-treated NIH 3T3 cells.

siPD-L1/pd blocks the immune checkpoint interaction between B16F10-OVA cells and T lymphocytes

The suppression of PD-L1 expression is expected to reactivate tumor-specific CTLs, which are suppressed by PD-1/PD-L1 interactions with B16F10 cells. To examine if silencing PD-L1 in B16F10 helps T lymphocytes to recognize and attack the target, we co-cultured OT-1 mouse splenocytes (which contain T lymphocytes) stimulated with ovalbumin (257–264) ($OVA_{257–264}$)-pulsed dendritic cells (DCs) and B16F10-OVA cells transfected with different treatments and examined the lysis and apoptosis of the B16F10-OVA cells. The stimulated splenocytes showed the most pronounced cytolytic activities against B16F10-OVA cells receiving siPD-L1/pd at all effector-to-target ratios (Figure 3a, b). The cells treated with siNeg/pd showed more lysis than PBS-treated cells, likely reflecting the B16F10-specific toxicity of pd complex, but not as much as siPD-L1/pd-treated ones. This result indicates that the sensitivity of siPD-L1/pd-treated cells to the splenocytes is mostly attributable to the silencing of PD-L1. Consistently, B16F10-OVA treated with siPD-L1/pd showed greater apoptotic cell populations than those treated with PBS or siNeg/pd (Figure 3c, d). These results confirm that siPD-L1/pd made B16F10-OVA cells susceptible to T lymphocytes by suppressing PD-L1 expression and blocking the immune checkpoint interactions with T lymphocytes.

siPD-L1/pd inhibits the proliferation of B16F10 cells

In addition to the effect on tumor-specific T-cell immunity, PD-1/PD-L1 interactions also have cancer cell-intrinsic functions that promote tumor survival and growth such as mTOR signaling.[9–10] Indeed, the PD-L1 expression in B16F10 cells was mirrored by the expression of p-S6K, an effector molecule of the mTOR pathway.[20] IFN-γ treatment induced a twofold increase of p-S6K expression (Figure 2c, d), followed by the increased levels of melanoma-specific gene products (Figure S3). With the siPD-L1/pd treatment, p-S6K level returned to the same level as the unstimulated control (Figure 2c, d).

siPD-L1/pd inhibited the proliferation of B16F10 cells. In the absence of IFN-γ treatment, pd and siNeg/pd reduced B16F10 cell proliferation (Figure 4), consistent with the earlier assessment (Figure 1f), although melanoma-specific gene production remained unchanged (Figure S3). siPD-L1/pd induced further reduction of B16F10 cell survival (Figure 4), followed by the reduction of melanoma-specific genes (Figure S3). The overall cell viability

increased with IFN-γ treatment, but the treatment effects showed a consistent trend, with pd and siRNA/pd reducing cell proliferation as compared to non-treated ones (Figure 4). In the overwhelming effect of IFN-γ, the net proliferation of pd- and siNeg/pd-treated cells was not different from the non-stimulated B16F10 cells. However, siPD-L1/pd counteracted the effect of IFN-γ, reducing the cell viability by 20% relative to the unchallenged B16F10 cells.

siPD-L1/pd attenuates B16F10 tumor growth in both immune-competent and immune-compromised mice

Therapeutic efficacy of siPD-L1/pd was evaluated by measuring tumor growth of B16F10-OVA tumors in immune-competent syngeneic C57BL/6 mice and immune-compromised Balb/c nude mice. A siRNA dose of 1.5 mg/kg was administered 5 times every three days (q3d) *via* tail vein. In C57BL/6 mice, the siPD-L1/pd-treated group showed a significantly delay in tumor growth compared with the PBS-treated group (Figure 5a, b). The siNeg/pd-treated group showed no significant difference from the PBS-treated group. The tumor specific growth rates (SGRs) of PBS-, siNeg/pd- and siPD-L1/pd-treated groups were 0.0796, 0.0752 and 0.0394, respectively.

A similar yet milder effect was seen in immune-compromised Balb/c nude mice. Tumor growth was significantly delayed in the siPD-L1/pd-treated group as compared with the PBS- or siNeg/pd-treated group (Figure 5c, d). Similar to the C57BL/6 model, siNeg/pd had no significant effect on tumor growth, which indicates that observed effect of siPD-L1/pd was not a non-specific effect of siRNA/pd but attributable to siPD-L1. The tumor SGRs of PBS-, siNeg/pd- and siPD-L1/pd-treated groups were 0.1027, 0.0979 and 0.0817, respectively.

The anti-tumor efficacy was evaluated with a lower dose of siRNA (0.75 mg/kg) and a greater interval with less frequency (3 times, every 5 days) in both animal models. Although the responses were relatively mild, consistent trends were observed in both C57BL/6 and Balb/c nude mice (Figure S4a).

siPD-L1/pd inhibits B16F10 tumor growth by both mTOR pathway suppression and immune checkpoint blockade

To confirm the silencing of PD-L1 by siPD-L1/pd complex, tumors were harvested at the completion of the study (2 days after the last treatment) and analyzed with western blotting. In both C57BL/6 and nude mice, the expressions of PD-L1 and p-S6K in B16F10-OVA tumors of the siPD-L1/pd-treated animals were significantly less than those of PBS- and siNeg/pd-treated groups (Figure 6). There were positive correlations between PD-L1 expression and S6K phosphorylation (p-S6K), p-S6K and tumor SGR, and PD-L1 and tumor SGR with the Pearson's coefficients of 0.9436, 0.8293, and 0.8756 (C57BL/6) and 0.9128, 0.7728, and 0.7433 (nude mice), respectively (Figure S5). This result is consistent with the implication of mTOR pathway in B16F10 tumor progression and supports its inhibition by siPD-L1/pd complex. Similar trends were seen with the animals treated with lower dose-treated animals (Figure S4b, c).

To evaluate the effect of siPD-L1/pd treatment on tumor-specific T-cell immunity, draining lymph nodes (DLNs) and spleens of the treated C57BL/6 mice were harvested, stimulated with $OVA_{275–264}$ and examined with respect to the IFN-γ production, which reflects the extent of CTL activation.[18] DLN cells and splenocytes of the siPD-L1/pd-treated animals produced 2.7 and 4.9 times more IFN-γ than the PBS-treated group, respectively (Figure 7). With additional GM-CSF that induces DC maturation, DLN cells and splenocytes of the siPD-L/pd-treated animals showed a 3.1 and 7.7 fold increase of IFN-γ production compared with the PBS-treated group. In both cases, the siNeg/pd-treated group showed no difference from the PBS-treated group. Immunophenotyping of tumors and DLNs also supported the enhancement of anti-tumor immunity due to the siPD-L1/pd-mediated immune checkpoint blockade. siPD-L1/pd-treated animals showed a significantly higher $CD8^+$ T cells population (4.56%) in tumors than PBS-treated (1.16%) or siNeg/pd-treated animals (1.46%) (Figure 8a), though with no significant change in CD69 expression (T cell activation marker) (Figure S6). $CD4^+$ T cell population in tumors remained constant irrespective of the treatment (Figure 8a); however, the expression of immunosuppressive regulatory T (T_{reg}) cell marker, Foxp3, was significantly decreased in the siPD-L1/pd-treated animals as compared to PBS-treated animals (Figure 8b, Figure S7). The siPD-L1/pd group showed increased ratios of $CD8^+$ T cells to $CD4^+Foxp3^+$ T cells and $CD4^+Foxp3^-$ T cells to $CD4^+Foxp3^+$ T cells in tumors as compared to the PBS group (Figure 8c). siPD-L1/pd-treated animals also showed greater expression of DC maturation markers (CD40 and CD86) in DLN cells as compared to PBS-treated animals (Figure 8d).

pd complex induces maturation of BMDCs

To test whether pd complex alone may affect the immune system in tumors, we treated BMDCs with the pd complex and each component (CLPEI and DS) and examined the expression of CD40 and CD86. BMDCs treated with pd complex showed a significant increase in the expression of CD40 and CD86 as compared with PBS-treated cells (Figure 9, Figure S8). An equivalent amount of CLPEI or DS induced no change.

DISCUSSION

On the basis of broad expression of PD-L1 in tumor microenvironment and its dual role in melanoma progression, we expected that suppression of PD-L1 by siRNA would effectively delay tumor growth. We used the CLPEI/DS (pd) complex as the carrier of siPD-L1 due to the safety and specific toxicity to $CD146^+$ tumor cells observed in our previous study.[14] The *in vitro* PD-L1 silencing by siPD-L1/pd complex was examined with IFN-γ-treated B16F10 melanoma and NIH 3T3 fibroblast cells. As expected from the previous study, siPD-L1/pd complex transfected $CD146^+$ B16F10 cells and decreased their expression of PD-L1 (Figure 2) but did not affect NIH 3T3 cells. The suppression of PD-L1 was accompanied by the reduction of p-S6K, an effector molecule of mTOR pathway.

The PD-L1 silencing brought about twofold effects on B16F10 cell proliferation. First, siPD-L1/pd restored cytotoxic activity of CTLs against tumors. PD-1/PD-L1 interaction maintains lymphocyte homeostasis and prevents normal tissue damages from excessive immune responses.[21] However, chronic antigen exposure, which occurs with cancer, leads to

persistent expression of PD-1 in tumor-infiltrating CTLs, and its interaction with ligand PD-L1 in the tumor microenvironment induces an exhausted or anergic state of T cells, impairing antitumor immune responses.[2, 22] Melanoma is one of the tumors that upregulates PD-L1 expression and responds well to PD-1/PD-L1 immune checkpoint blockade[2, 5, 23]; consistently, the suppression of PD-L1 by siPD-L1/pd restored the activity of melanoma-specific T cells. We confirmed this activity *in vitro* from the increased lysis and apoptosis of siPD-L1/pd-treated B16F10-OVA cells by the stimulated OT-1 splenocytes (Figure 3). Second, siPD-L1/pd suppressed the induction of protumorigenic mTOR signaling pathway. Traditionally, mTOR activation is known to be an upstream, post-transcriptional regulator of the expression of PD-L1,[24–29] but recent studies also demonstrate that tumor-intrinsic PD-1/PD-L1 interaction activates the effectors of mTOR signaling pathway and promotes tumor growth.[9–10] Consistently, we found that siPD-L1/pd suppressed the expression of p-S6K (Figure 2c, d), the growth of B16F10 cells in monoculture (Figure 4) and the expression of melanoma-specific genes such as Trp1, Trp2, gp100 and Tyr.

The dual function of siPD-L1/pd is reflected *in vivo*. The intravenously injected siPD-L1/pd complex attenuated tumor growth significantly in both immune-competent C57BL/6 mice and immune-compromised Balb/c nude mice (Figure 5). The siPD-L1/pd treatment reduced the expression of PD-L1 and p-S6K in tumors (Figure 6) as demonstrated *in vitro* (Figure 2). Positive correlations among PD-L1 expression, S6K phosphorylation and Tumor SGR were observed in both mouse models. These correlations indicate that siPD-L1/pd suppressed mTOR-mediated protumorigenic signaling, consistent with the anti-tumor effect observed in the absence of functional adaptive immunity. We also confirmed the effect of siPD-L1/pd on tumor-specific T cell immunity. Cells were isolated from the DLNs and the spleen, which represent direct secondary lymphoid organs and an indirect secondary lymphoid organ, respectively, and examined with respect to their ability to produce IFN-γ, a marker of CTL activation. The DLN cells and splenocytes of the siPD-L1/pd-treated C57BL/6 mice produced a greater amount of IFN-γ than the PBS-treated group upon incubation with tumor antigen (Figure 7), indicating the presence of active tumor-specific CTLs in both lymphoid organs. The enhancement of anti-tumor immunity by siPD-L1/pd was also confirmed by immunophenotyping of tumors, which demonstrated a greater population of tumor-infiltrating $CD8^+$ T cells and an increased ratio of $CD8^+$ T cells to $CD4^+Foxp3^+$ T cells (Figure 8a–c). Moreover, siPD-L1/pd induced the maturation of DCs in DLNs, consistent with the expression of PD-L1 in DCs and inhibitory effect of PD-1/PD-L1 interaction on DC maturation.[30–31] Nevertheless, the effect on DCs was modest as compared to those involving siPD-L1/pd-treated B16F10 cells, most likely due to the limited transfection of DCs.

In this study, we focused on the effect of siPD-L1/pd on B16F10 cells and their interaction with CTLs, but it is also possible that siPD-L1/pd affected a broader population of cells. Contrary to *in vitro* observations, pd complex itself did not show prominent melanoma-specific toxicity *in vivo* (Figure 5, Figure S5), likely due to additional protumorigenic factors in the tumor microenvironment. However, we cannot rule out immune-modulatory effects of the pd complex in the tumor microenvironment. For example, PEI (precursor to CLPEI of the pd complex) activated tumor-associated dendritic cells *via* multiple toll-like receptors including TLR5 and reversed their tolerogenic phoenotype.[32] Indeed, the pd complex induced maturation of DCs, while each component did not (Figure 9). Given that

the extent of CLPEI interaction with DCs was comparable irrespective of DS (Figure S9), it is not simply the amount of CLPEI that drove the maturation of DCs. In future studies, it will be worthwhile to investigate how pd complex stimulates the immune system in the tumor microenvironment and synergizes the effect of siPD-L1.

While this study finds PD-L1 to be a promising therapeutic target for melanoma treatment, we note that an earlier study saw no significant effect of anti-PD-L1 antibody on tumor growth in a similar animal model (B16 tumors in C57BL/6 mice).[31] This study reported that anti-PD-L1 antibody was only effective when it was combined with additional immunization with antigen-primed dendritic cells and replacement of T cells.[31] Although systematic comparison remains to be done, we suspect that siPD-L1/pd may have had an advantage over anti-PD-L1 antibody in preventing *de novo* production of PD-L1 and thus provided an effective blockade of additional checkpoint interactions. Another notable aspect of this study is that siPD-L1/pd was delivered to tumors by intravenous injection. Systemic delivery of siRNA to organs other than the liver has proven difficult due to the universal challenges in nucleic acid delivery, such as insufficient stability in serum, non-specific uptake by the reticuloendothelial system, insufficient uptake by target cells.[33] We previously observed that gene/CLPEI-polysaccharide complexes had greater serum stability than those based on commercial polymers[15] and thus speculate that the improved stability has contributed to the systemic delivery of siRNA. This suggests that additional efforts to improve circulation stability of the delivery system may help siRNA to provide clinical benefits in systemic cancer therapy.

CONCLUSION

We evaluated dual inhibitory effects of siPD-L1 on melanoma growth using a polyelectrolyte complex consisting of disulfide-crosslinked polyethyleneimine and dermatan sulfate as a melanoma-specific gene carrier. siPD-L1/pd complex entered B16F10 cells in a cell-specific manner and suppressed the expression of PD-L1 and melanoma-specific genes. The siPD-L1/pd complex showed anti-tumor effects in both immune-competent C57BL/6 mice and immune-compromised Balb/c nude mice, indicating that it affects not only the anti-tumor immunity but also intrinsic tumorigenicity in B16F10 tumors. Analysis of treated tumors supports that siPD-L1 restored antitumor immunity of CTLs by blocking the immune checkpoint interaction and inhibited tumorigenic mTOR signaling pathway by suppressing the phosphorylation of S6K. Further investigation is warranted for siPD-L1/pd as a potential cancer therapy.

EXPERIMENTAL SECTION

Materials

A HCl salt form of linear polyethylenimine (LPEI, MW: 2.5 kDa) was purchased from Polysciences (Warrington, PA, USA). Chondroitin sulfate B sodium salt (dermatan sulfate sodium salt from porcine intestinal mucosa), 3,3′-dithiodipropionic acid di(N-hydroxysuccinimide ester) (DSP), 3-(4,5-dimethyl-2-thiazolyl)-2,5-diphenyl-2H-tetrazolium bromide (MTT), ovalbumin (257–264) chicken ($OVA_{275–264}$), 2-Mercaptoethanol were purchased from Sigma-Aldrich (St. Louis, MO, USA). Carbon type-B (400 mesh) copper

grid was purchased from Ted Pella, Inc (Redding, CA, USA). Uranyl acetate dihydrate was purchased from Electron Microscopy Sciences (Hatfield, PA, USA). siRNA specific for the mouse *pdcd1lg1* mRNA (sense, 5′-CCCACAUAAAAAACAGUUGTT-3′; antisense, 5′-CAACUGUUUUUUAUGUGGGTT-3′), negative siRNA (sense, 5′-UGAAGUUGCACUUGAAGUCdTdT-3′; antisense, 5′-GACUUCAAGUGCAACUUCAdTdT-3′) and Cy5-labeled negative siRNA were purchased from IDT (Coralville, Iowa, USA). Mouse B7-H1/PD-L1 Antibody (af1019) and mouse interferon-gamma (IFN-γ) Quantikine ELISA Kit were purchased from R&D systems (Minneapolis, MN, USA), and phospho-S6 Ribosomal Protein (Ser235/236) Antibody (2211) was from Cell signaling (Danvers, MA, USA). Recombinant murine IFN-γ, GM-CSF and IL-4 were purchased from Peprotech (Rocky Hill, NJ, USA). CellTracker Deep Red Dye and Lipofectamine 2000 Transfection Reagent were purchased from Thermo Fisher Scientific Inc (Rockford, IL, USA). Annexin-V-FLUOS staining kit was purchased from Roche (Basel, Switzerland). Mouse Trp-1 primer (forward, 5′ CCCCTAGCCTATATCTCCCTTTT-3′; reverse, 5′-TACCATCGTGGGGATAATGGC-3′), mouse Trp-2 primer (forward, 5′-GTCCTCCACTCTTTTACAGACG-3′; reverse, 5′-ATTCGGTTGTGACCAATGGGT-3′), mouse gp100 primer (forward, 5′-ACATTTCATCACCAGCAGGGTGCC-3′; reverse, 5′-AACAAGTGGGTGCTGGCC-3′), mouse Tyr primer (forward, 5′-CTCTGGGCTTAGCAGTAGGC-3′; reverse, 5′-GCAAGCTGTGGTAGTCGTCT-3′) were purchased from Bioneer (Daejeon, Korea). RNeasy® Plus Mini Kit was purchased from Qiagen (Valencia, CA, USA). High Capacity RNA-to-cDNA Kit was purchased from Applied Biosystems (Foster City, CA, USA). APC anti-mouse CD8a antibody, APC anti-mouse CD4 antibody, PE anti-mouse CD69 antibody, PE anti-mouse/rat/human FOXP3 antibody, FITC anti-mouse CD11c antibody, APC anti-mouse CD11c antibody, APC anti-mouse CD40 antibody, PE anti-mouse CD40 antibody, APC anti-mouse CD86 antibody, PE anti-mouse CD86 antibody, FITC Armenian hamster anti-mouse IgG isotype control antibody, APC rat anti-mouse igG2a κ isotype control antibody, APC Rat anti-mouse IgG2b κ isotype control antibody, APC Armenian hamster anti-mouse IgG isotype control antibody, PE Armenian Hamster anti-mouse IgG isotype control antibody, PE Mouse IgG1 κ isotype control (ICFC) antibody, PE Rat anti-mouse IgG2a κ isotype control antibody and True-Nuclear™ Transcription Factor Buffer Set were purchased from Biolegend (San diego, CA, USA). Purified rat anti-mouse CD16/CD32 (Mouse BD Fc Block™) was purchased from BD Biosciences (San jose, CA, USA). Tumor Dissociation Kit was purchased from Miltenyi Biotec (Bergisch Gladbach, Germany).

Cell culture

The mouse melanoma (B16F10) and mouse fibroblast (NIH 3T3) were obtained from the American Type Culture Collection (ATCC, Rochkville, MD, USA). Mouse B16F10-OVA cell line, a B16F10 cell line that stably expresses chicken ovalbumin (OVA), was a gift of the Prof. Seung-Hyo Lee at Korea Advanced Institute of Science and Technology (KAIST, Daejeon, Korea). These cells were cultured in Dulbecco's Modified Eagle's Medium (DMEM) with 10% fetal bovine serum and 1% antibiotic-antimycotic (Welgene Inc., Daegu, Korea). B16F10 and NIH 3T3 were passaged when cells reached 80% confluence using 0.5% trypsin-EDTA (Welgene Inc.). Primary mouse DLN cells, splenocytes, and bone marrow-derived dendritic cells (BMDCs) were cultured in RPMI-1640 medium

supplemented with 10% fetal bovine serum and 1% antibiotic-antimycotic and used in 10 days.

Animals

C57BL/6 and BALB/c-nude mice (male, 5 weeks) were purchased from Narabiotech (Seoul, Korea). C57BL/6-Tg(TcraTcrb)1100Mjb/J mice, the source of OVA $_{257–264}$-specific (OT-1) T cells, were purchased from the Jackson Laboratory (Bar Harbor, ME, USA).

Preparation and characterization of siRNA/pd complex

Disulfide-crosslinked low molecular weight linear polyethylenimine (CLPEI) was synthesized as previously described [15]. First, CLPEI was incubated with siRNA in various weight ratios for 30 min in phosphate buffered saline (PBS, pH 7.4) at room temperature. After the incubation, the formation of binary complexes was confirmed by 2% agarose gel electrophoresis. The siRNA/CLPEI binary complexes were incubated with dermatan sulfate (DS) in various weight ratios for 20 min at room temperature. The formed siRNA/CLPEI/DS ternary complex was called siRNA/pd complex. The size and zeta potential of the siRNA/pd complexes were measured in pH 7.4 PBS with a Malvern NanoZS Zeta-sizer (Malvern, UK). The siRNA/pd complex was visualized by TEM. Ten microliters of siRNA/pd complex (equivalent to 3 μg CLPEI) was loaded on carbon type-B copper grid and air-dried for 3 min. After rinsing with deionized water for 1 min, the samples were stained with 2% uranyl acetate dihydrate for 30 s. The grid was dried overnight and analyzed with FEI Tecnai G2 F20 Transmission Electron Microscope (Hilsboro, OR, USA) at an accelerated voltage of 200 kV.

Cellular uptake of siRNA/pd complexes

For the evaluation of cellular uptake of siRNA complexes by fluorescence microscopy and flow cytometry, siRNA/pd complex and siRNA/Lipo were prepared with Cy5-labeled siRNA. B16F10 and NIH 3T3 cells were plated in Φ35 glass bottom dishes at a density of 5×10^4 cells per dish with 1 mL culture medium and incubated for 24 h. The cells were incubated with siRNA complexes equivalent to 100 nM siRNA-Cy5 in serum-free medium for 6 h (siRNA-Cy5/pd) or 4 h (siRNA-Cy5/Lipo). For fluorescence imaging, the cells were fixed with 4% paraformaldehyde (PFA) for 5 min, rinsed twice, counterstained with 4′,6-diamidino-2-phenylindole (DAPI) and observed with an Olympus fluorescence microscope IX81 (Tokyo, Japan). For flow cytometry, the cells were trypsinized and analyzed with a Guava® easyCyte Flow Cytometer (Billerica, MA, USA).

Expression and silencing of PD-L1

B16F10 and NIH 3T3 cells were plated in 6-well plates at a density of 10^5 cells per plate with 3 mL culture medium and incubated for 24 h. For expression of PD-L1, the cells were treated with 25 ng/mL of IFN-γ for 4 h, incubated for additional 0, 12, 24, and 48 h, and lysed using a cell lysis buffer containing 1% protease inhibitor. To evaluate silencing of PD-L1, the cells were pre-treated with 25 ng/mL of IFN-γ for 4 h and transfected with siPD-L1/pd or siNeg/pd (pd complex containing siRNA irrelevant to PD-L1) equivalent to 100 nM

siRNA in serum-free medium for 6 h. After 48 h incubation, the cells were lysed for western blotting.

For western blotting, the lysates were centrifuged at 12,000 ×g for 20 min at 4 °C to separate a supernatant. The total protein content in the supernatant was quantified by the BCA assay, and samples corresponding 10 mg of protein were mixed with sodium dodecyl sulfate (SDS) gel-loading buffer and incubated for 5 min at 95 °C. Samples corresponding to 100 μg of proteins were separated by 10% SDS-polyacrylamide gel electrophoresis and transferred onto polyvinylidene fluoride (PVDF) membrane. The membranes were blocked at room temperature in 5% nonfat dried milk containing TBS-T solution (pH 7.4, 20 mM Tris, 150 mM NaCl and 0.05% Tween 20). After 1 h, the membranes were incubated with a recommended concentration of PD-L1 and β-actin antibody for 24 h at 4 °C. The membranes were washed 3 times and incubated with secondary IgG-HRP antibody for 1 h at room temperature. After incubation with secondary antibody, the membranes were washed 3 times, and protein bands were detected with the SuperSignal™ West Femto Maximum Sensitivity Substrate (Rockford, IL, USA).

In vitro cytolytic activity of stimulated OT-1 splenocytes on siPDL1/pd-transfected B16F10-OVA cells

Bone marrow cells were obtained from C57BL/6 mice using a syringe according to the method described in the literature.[34] After overnight incubation of the cell suspension at 37 °C, non-adherent cells were separated and incubated with 20 ng/mL granulocyte macrophage colony-stimulating factor (GM-CSF), 20 ng/mL of interleukin 4 (IL-4) and 0.1% 2-mercaptoethanol to differentiate into DCs. On day 3 and 5, the medium were replaced with fresh cytokines. On day 7, cell differentiation into DCs was confirmed by CD11c staining. The BMDCs were pulsed with 10 μg/mL $OVA_{257–264}$ peptide overnight. Separately, splenocytes were derived from the spleen of OT-1 mice. The isolated splenocytes were incubated with the $OVA_{257–264}$-pulsed BMDCs at a 10:1 ratio for 5 days.

The effects of the stimulated OT-1 splenocytes on B16F10-OVA cells were evaluated based on the extents of B16F10-OVA cell lysis and apoptosis. B16F10-OVA cells were stained with CellTracker™ Deep Red and plated in a 12-well plate. The Deep Red-stained B16F10-OVA cells were transfected with siPD-L1/pd or siNeg/pd complexes in serum-free medium for 6 h. Two days after transfection, the B16F10-OVA (target cells) were co-cultured with the stimulated OT-1 splenocytes (effector cells) at various effector-to-target (E/T) ratios in a 12-well plate for 4 h. For the measurement of cytolytic activity of OT-1 splenocytes, the Deep Red fluorescence intensity (FI) of the medium, corresponding to the released cytoplasmic contents, was imaged by IVIS Spectrum system (Xenogen Corporation, USA). The percent specific lysis of B16F10-OVA cells was calculated as 100 × (sample FI - spontaneous FI)/(maximal FI), where the spontaneous and maximum FI refer to those of B16F10 cells cultured in complete medium alone and in 10% SDS, respectively. For the detection of B16-F10 cell apoptosis by OT-1 splenocytes, B16F10-OVA cells were stained with annexin V-fluorescein isothiocyanate (FITC) conjugate and propidium iodide (PI) using the annexin-V-FLUOS staining kit according to the manufacturer's instruction. The cells were suspended in 100 μL of annexin-V-FLUOS labeling solution containing annexin-V-

FITC and PI. After 10 min incubation time at room temperature, the stained cells were rinsed with PBS and analyzed with Guava® easyCyte Flow Cytometer. The percentage of cells undergoing apoptosis was determined by dual-color analysis.

In vitro effect of siPDL-1/pd complex on melanoma-specific gene expression

To observe the effect of PD-L1 silencing on the melanoma specific gene expression, 10^5 of B16F10 cells were seeded in a Φ60 cell culture dish and maintained for 24 h. Then, siRNA/pd or pd complex equivalent to 1.5 μg/mL siRNA and/or 3 μg/mL CLPEI, suspended in serum-free RPMI medium, was added to cells. After 6 h, the transfection medium was replaced with complete growth medium, and cells were incubated for additional 48 h. Total RNA was isolated from the transfected B16F10 cells using a RNeasy® Plus Mini Kit according to the manufacturer's recommendation. For DNA amplification, cDNA was formed using 1 μg of total RNA and a High Capacity RNA-to-cDNA kit. RT-PCR was carried out with the cDNA with the following thermal cycling conditions: denaturation: 1 cycle 94 °C for 2 min, PCR amplification; 20 cycles for Trp1 and HPRI, 25 cycles for Trp2, gp100 and Tyr at 94 °C for 20 s, at 60 °C for 30 s, and at 72 °C for 30 s, final extension; 1 cycle 70 °C for 5 min. The PCR products were separated on a 2% agarose gel by electrophoresis.

In vitro effect of siPDL-1/pd complex on cell proliferation

Cell viability was tested using the Thiazolyl Blue Tetrazolium Bromide (MTT) assay. B16F10 cells were plated in 48-well plates at a density of 2×10^4 cells per dish with 200 μL culture medium and incubated for 24 h. The cells were treated with 25 ng/mL of IFN-γ or PBS for 4 h and transfected with siRNA/pd or pd complex equivalent to 1.5 μg/mL siRNA and/or 3 μg/mL CLPEI in serum-free medium for 6 h. For MTT assay, the medium was replaced with 0.5 mg/mL of MTT solution in serum-free RPMI medium. After 1 h incubation, the MTT solution was replaced by DMSO, and the plate were shaken to complete dissolution of formazan. The formazan solution was transferred to a 96-well plate and analyzed at 450 nm using a VERSAmax™ microplate reader (Sunnyvale, CA, USA).

In vivo effects of siPDL-1/pd on tumor progression in immune-competent C57BL/6 and immune-compromised Balb/c nude mice

All experiments with live animals were performed with the permission of the institutional committee (approval number: 2017-006), in compliance with the relevant laws and institutional guidelines of Korea Institute of Science and Technology (KIST). Tumor-bearing mice were prepared by subcutaneous injection of 10^6 B16F10-OVA cells suspended in 100 μL growth medium into the left flank of immune-competent C57BL/6 and immune-compromised Balb/c nude mice (male, 5 weeks old). When the tumor size reached 50 mm^3, animals received intravenous injection of PBS, siNeg/pd (30 μg siNeg + 60 μg CLPEI + 120 μg DS), and siPD-L1/pd (30 μg siPD-L1 + 60 μg CLPEI + 120 μg DS) *via* tail vein. The treatment was repeated 4 more times with a 3 day interval. Tumor size was monitored every two days. The SGR was calculated as $(\log V_2 - \log V_1)/(t_2 - t_1)$, where V is tumor volume in mm^3 and t is time in days.[35]

To examine the effect of siPD-L1/pd on PD-L1 and pS6K expression in tumors, animals were sacrificed 26 days post-tumor inoculation, and the B16F10-OVA tumors were harvested. The tumors were homogenized using a Wisemix homogenizer (Seongbuk-gu, Seoul, Korea) and lysed with a lysis buffer containing 1% protease inhibitor. The tissue lysates were analyzed with the western blot as described previously. The Pearson correlation coefficient was calculated between the tumor SGR and the relative expression of PD-L1 or pS6K in B16F10-OVA tumors using GraphPad Prism 7 (La Jolla, CA).

In vivo effects of siPDL-1/pd on anti-tumor immunity

To evaluate the effect of siPD-L1/pd on tumor-specific T-cell immunity, DLN and spleen were harvested from the treated C57BL/6 mice on day 26 to isolate DLN cells and splenocytes, respectively. Erythrocytes were eliminated from each preparation using a RBC lysis buffer. Two million DLN cells and 2×10^7 splenocytes were plated with 10 μg/mL of $OVA_{257–264}$ peptide, in the absence and presence of 20 ng/mL of GM-CSF, for 48 h. The level of IFN-γ in the medium was measured by ELISA.

Tumors and DLNs were harvested from the treated C57BL/6 mice on day 26 were subjected to immunophenotyping. Tumors were cut into small pieces (2–3 mm in diameter) and dissociated with the Tumor Dissociation Kit according to the manufacturer's instruction. After eliminating RBCs from the dissociated tumors, suspending cells were spun down for 10 min at 300 ×g, resuspended in PBS (10^6 cells per 100 μL), and treated with the Mouse BD Fc Block for 5 min. The cells were labeled with APC anti-mouse CD8a, PE anti-mouse CD69, APC anti-mouse CD4 and isotype control antibodies for 1 h at 4 °C. After fixing and permeabilizing the labeled suspension cells with the True-Nuclear™ Transcription Factor Buffer Set, Foxp3 transcription factor was labeled with PE anti-mouse/rat/human FOXP3 and isotype control antibodies for 1 h at room temperature. DLN cells were prepared in the same way except for the dissociation step and stained with FITC or APC anti-mouse CD11c, APC or PE anti-mouse CD40, APC or PE anti-mouse CD86 and isotype control antibodies. The stained cells were rinsed with 1 mL of PBS, resuspended in 100 μL of PBS, and analyzed with a Guava® easyCyte Flow Cytometer (Billerica, MA, USA) to detect $CD8a^+CD69^+$ and $CD4^+Foxp3^+$ populations for tumor cells and $CD11c^+CD40^+$ and $CD11c^+CD86^+$ populations for DLN cells.

In vitro effect of pd complex on DC maturation

BMDCs were plated in a 6-well plate at a density of 10^6 cells and treated with 3 μg/mL of CLPEI, 6 μg/mL of DS, and pd complex (DS/CLPEI ratio of 2) equivalent to 3 μg/mL CLPEI for 24 h. The treated BMDCs were stained in the same manner as above and analyzed with a Guava® easyCyte Flow Cytometer (Billerica, MA, USA) to detect $CD11c^+CD40^+$ and $CD11c^+CD86^+$ populations.

Statistical analysis

All data were analyzed using GraphPad Prism 7 (La Jolla, CA) with ANOVA followed by the recommended tests for multiple comparisons. SGR was calculated for each animal, and the groups were compared with ANOVA and Tukey's test for multiple comparisons. A value of $p < 0.05$ was considered statistically significant.

Supplementary Material

Refer to Web version on PubMed Central for supplementary material.

Acknowledgments

The authors acknowledge the support of NSF DMR-1056997, NIH R01 CA199663, NIH R01 EB017791 and the Intramural Research Program (Global RNAi Carrier Initiative) of KIST.

References

1. Nguyen LT, Ohashi PS. Clinical Blockade of PD1 and Lag3-Potential Mechanisms of Action. Nat Rev Immunol. 2015; 15:45–56. [PubMed: 25534622]
2. Pardoll DM. The Blockade of Immune Checkpoints in Cancer Immunotherapy. Nat Rev Cancer. 2012; 12:252–264. [PubMed: 22437870]
3. He J, Hu Y, Hu M, Li B. Development of PD-1/PD-L1 Pathway in Tumor Immune Microenvironment and Treatment for Non-Small Cell Lung Cancer. Sci Rep. 2015; 5:13110. [PubMed: 26279307]
4. Hamid O, Robert C, Daud A, Hodi FS, Hwu WJ, Kefford R, Wolchok JD, Hersey P, Joseph RW, Weber JS, Dronca R, Gangadhar TC, Patnaik A, Zarour H, Joshua AM, Gergich K, Elassaiss-Schaap J, Algazi A, Mateus C, Boasberg P, et al. Safety and Tumor Responses with Lambrolizumab (Anti–PD-1) in Melanoma. N Engl J Med. 2013; 369:134–144. [PubMed: 23724846]
5. Brahmer JR, Tykodi SS, Chow LQM, Hwu WJ, Topalian SL, Hwu P, Drake CG, Camacho LH, Kauh J, Odunsi K, Pitot HC, Hamid O, Bhatia S, Martins R, Eaton K, Chen S, Salay TM, Alaparthy S, Grosso JF, Korman AJ, et al. Safety and Activity of Anti–PD-L1 Antibody in Patients with Advanced Cancer. N Engl J Med. 2012; 366:2455–2465. [PubMed: 22658128]
6. Wolchok JD, Kluger H, Callahan MK, Postow MA, Rizvi NA, Lesokhin AM, Segal NH, Ariyan CE, Gordon RA, Reed K, Burke MM, Caldwell A, Kronenberg SA, Agunwamba BU, Zhang X, Lowy I, Inzunza HD, Feely W, Horak CE, Hong Q, et al. Nivolumab Plus Ipilimumab in Advanced Melanoma. N Engl J Med. 2013; 369:122–133. [PubMed: 23724867]
7. Khoja L, Butler MO, Kang SP, Ebbinghaus S, Joshua AM. Pembrolizumab. J Immunother Cancer. 2015; 3:36. [PubMed: 26288737]
8. Mahoney KM, Freeman GJ, McDermott DF. The Next Immune-Checkpoint Inhibitors: PD-1/PD-L1 Blockade in Melanoma. Clin Ther. 2015; 37:764–782. [PubMed: 25823918]
9. Kleffel S, Posch C, Barthel Steven R, Mueller H, Schlapbach C, Guenova E, Elco Christopher P, Lee N, Juneja Vikram R, Zhan Q, Lian Christine G, Thomi R, Hoetzenecker W, Cozzio A, Dummer R, Mihm Martin C Jr, Flaherty Keith T, Frank Markus H, Murphy George F, Sharpe Arlene H, et al. Melanoma Cell-Intrinsic PD-1 Receptor Functions Promote Tumor Growth. Cell. 2015; 162:1242–1256. [PubMed: 26359984]
10. Clark CA, Gupta H, Sareddy GR, Pandeswara S, Lao S, Yuan B, Drerup JM, Padron A, Conejo-Garcia JR, Murthy K, Liu Y, Turk MJ, Thedieck K, Hurez V, Li R, Vadlamudi RK, Curiel TJ. Tumor-Intrinsic PD-L1 Signals Regulate Cell Growth, Pathogenesis and Autophagy in Ovarian Cancer and Melanoma. Cancer Res. 2016; 76:6964–6974. [PubMed: 27671674]
11. Dolina JS, Sung SS, Novobrantseva TI, Nguyen TM, Hahn YS. Lipidoid Nanoparticles Containing PD-L1 siRNA Delivered *in Vivo* Enter Kupffer Cells and Enhance Nk and CD8(+) T Cell-Mediated Hepatic Antiviral Immunity. Mol Ther Nucleic Acids. 2013; 2:e72. [PubMed: 23423360]
12. Teo PY, Yang C, Whilding LM, Parente-Pereira AC, Maher J, George AJ, Hedrick JL, Yang YY, Ghaem-Maghami S. Ovarian Cancer Immunotherapy Using PD-L1 siRNA Targeted Delivery from Folic Acid-Functionalized Polyethylenimine: Strategies to Enhance T Cell Killing. Adv Healthc Mater. 2015; 4:1180–1189. [PubMed: 25866054]
13. Lee SJ, Yook S, Yhee JY, Yoon HY, Kim MG, Ku SH, Kim SH, Park JH, Jeong JH, Kwon IC, Lee S, Lee H, Kim K. Co-Delivery of VEGF and Bcl-2 Dual-Targeted siRNA Polymer Using a Single

Nanoparticle for Synergistic Anti-Cancer Effects *in Vivo*. J Control Release. 2015; 220:631–641. [PubMed: 26307351]

14. Kim BK, Kim D, Kwak G, Yhee JY, Kwon IC, Kim SH, Yeo Y. Polyethylenimine-Dermatan Sulfate Complex, a Bioactive Biomaterial with Unique Toxicity to CD146-Positive Cancer Cells. ACS Biomater Sci Eng. 2017; 3:990–999.
15. Xu P, Quick G, Yeo Y. Gene Delivery through the Use of a Hyaluronate-associated Intracellularly Degradable Cross-linked Polyethyleneimine. Biomaterials. 2009; 30:5834–5843. [PubMed: 19631979]
16. Breunig M, Lungwitz U, Liebl R, Goepferich A. Breaking up the Correlation between Efficacy and Toxicity for Nonviral Gene Delivery. Proc Natl Acad Sci US A. 2007; 104:14454–14459.
17. Spranger S, Spaapen RM, Zha Y, Williams J, Meng Y, Ha TT, Gajewski TF. Up-Regulation of PD-L1, IDO, and T_{regs} in the Melanoma Tumor Microenvironment is Driven by CD^{8+} T Cells. Sci Transl Med. 2013; 5:200ra116.
18. Mandai M, Hamanishi J, Abiko K, Matsumura N, Baba T, Konishi I. Dual Faces of IFNgamma in Cancer Progression: A Role of PD-L1 Induction in the Determination of Pro- and Antitumor Immunity. Clin Cancer Res. 2016; 22:2329–2334. [PubMed: 27016309]
19. Abiko K, Matsumura N, Hamanishi J, Horikawa N, Murakami R, Yamaguchi K, Yoshioka Y, Baba T, Konishi I, Mandai M. IFN-Gamma from Lymphocytes Induces PD-L1 Expression and Promotes Progression of Ovarian Cancer. Br J Cancer. 2015; 112:1501–1509. [PubMed: 25867264]
20. [accessed on March 1, 2017] RPS6KB1 ribosomal protein S6 kinase B1 [Homo sapiens (human)]. https://www.ncbi.nlm.nih.gov/gene/6198
21. Topalian SL, Drake CG, Pardoll DM. Targeting the PD-1/B7-H1(PD-L1) Pathway to Activate Anti-Tumor Immunity. Curr Opin Immunol. 2012; 24:207–212. [PubMed: 22236695]
22. Ahmadzadeh M, Johnson LA, Heemskerk B, Wunderlich JR, Dudley ME, White DE, Rosenberg SA. Tumor Antigen-Specific CD8 T Cells Infiltrating the Tumor Express High Levels of PD-1 and Are Functionally Impaired. Blood. 2009; 114:1537–1544. [PubMed: 19423728]
23. Topalian SL, Hodi FS, Brahmer JR, Gettinger SN, Smith DC, McDermott DF, Powderly JD, Carvajal RD, Sosman JA, Atkins MB, Leming PD, Spigel DR, Antonia SJ, Horn L, Drake CG, Pardoll DM, Chen L, Sharfman WH, Anders RA, Taube JM, et al. Safety and Activity Immune Correlates of Anti-PD-1 Antibody in Cancer. N Engl J Med. 2012; 366:2443–2454. [PubMed: 22658127]
24. Parsa AT, Waldron JS, Panner A, Crane CA, Parney IF, Barry JJ, Cachola KE, Murray JC, Tihan T, Jensen MC, Mischel PS, Stokoe D, Pieper RO. Loss of Tumor Suppressor Pten Function Increases B7-H1 Expression and Immunoresistance in Glioma. Nat Med. 2007; 13:84–88. [PubMed: 17159987]
25. Holets LM, Carletti MZ, Kshirsagar SK, Christenson LK, Petroff MG. Differentiation-Induced Post-Transcriptional Control of B7-H1 in Human Trophoblast Cells. Placenta. 2009; 30:48–55. [PubMed: 19010538]
26. Rosborough BR, Raich-Regue D, Matta BM, Lee K, Gan B, DePinho RA, Hackstein H, Boothby M, Turnquist HR, Thomson AW. Murine Dendritic Cell Rapamycin-Resistant and Rictor-Independent Mtor Controls IL-10, B7-H1, and Regulatory T-Cell Induction. Blood. 2013; 121:3619–3630. [PubMed: 23444404]
27. Zhang Y, Zhang J, Xu K, Xiao Z, Sun J, Xu J, Wang J, Tang Q. PTEN/PI3K/mTOR/B7-H1 Signaling Pathway Regulates Cell Progression and Immuno-Resistance in Pancreatic Cancer. Hepatogastroenterology. 2013; 60:1766–1772. [PubMed: 24624456]
28. Ritprajak P, Azuma M. Intrinsic and Extrinsic Control of Expression of the Immunoregulatory Molecule Pd-L1 in Epithelial Cells and Squamous Cell Carcinoma. Oral Oncol. 2015; 51:221–228. [PubMed: 25500094]
29. Lastwika KJ, Wilson W 3rd, Li QK, Norris J, Xu H, Ghazarian SR, Kitagawa H, Kawabata S, Taube JM, Yao S, Liu LN, Gills JJ, Dennis PA. Control of PD-L1 Expression by Oncogenic Activation of the AKT-mTOR Pathway in Non-Small Cell Lung Cancer. Cancer Res. 2016; 76:227–238. [PubMed: 26637667]

30. Kuipers H, Muskens F, Willart M, Hijdra D, van Assema FB, Coyle AJ, Hoogsteden HC, Lambrecht BN. Contribution of the PD-1 Ligands/PD-1 Signaling Pathway to Dendritic Cell-Mediated CD^{4+} T Cell Activation. Eur J Immunol. 2006; 36:2472–2482. [PubMed: 16917960]

31. Pilon-Thomas S, Mackay A, Vohra N, Mule JJ. Blockade of Programmed Death Ligand 1 Enhances the Therapeutic Efficacy of Combination Immunotherapy against Melanoma. J Immunol. 2010; 184:3442–3449. [PubMed: 20194714]

32. Cubillos-Ruiz JR, Engle X, Scarlett UK, Martinez D, Barber A, Elgueta R, Wang L, Nesbeth Y, Durant Y, Gewirtz AT, Sentman CL, Kedl R, Conejo-Garcia JR. Polyethylenimine-Based siRNA Nanocomplexes Reprogram Tumor-Associated Dendritic Cells *via* TLR5 to Elicit Therapeutic Antitumor Immunity. J Clin Invest. 2009; 119:2231–2244. [PubMed: 19620771]

33. Zhang Y, Satterlee A, Huang L. *In Vivo* Gene Delivery by Nonviral Vectors: Overcoming Hurdles? Mol Ther. 2012; 20:1298–304. [PubMed: 22525514]

34. Matheu MP, Sen D, Cahalan MD, Parker I. Generation of Bone Marrow Derived Murine Dendritic Cells for Use in 2-Photon Imaging. J Vis Exp. 2008; 17:e773.

35. Mehrara E, Forssell-Aronsson E, Ahlman H, Bernhardt P. Specific Growth Rate *versus* Doubling Time for Quantitative Characterization of Tumor Growth Rate. Cancer Res. 2007; 67:3970–3975. [PubMed: 17440113]

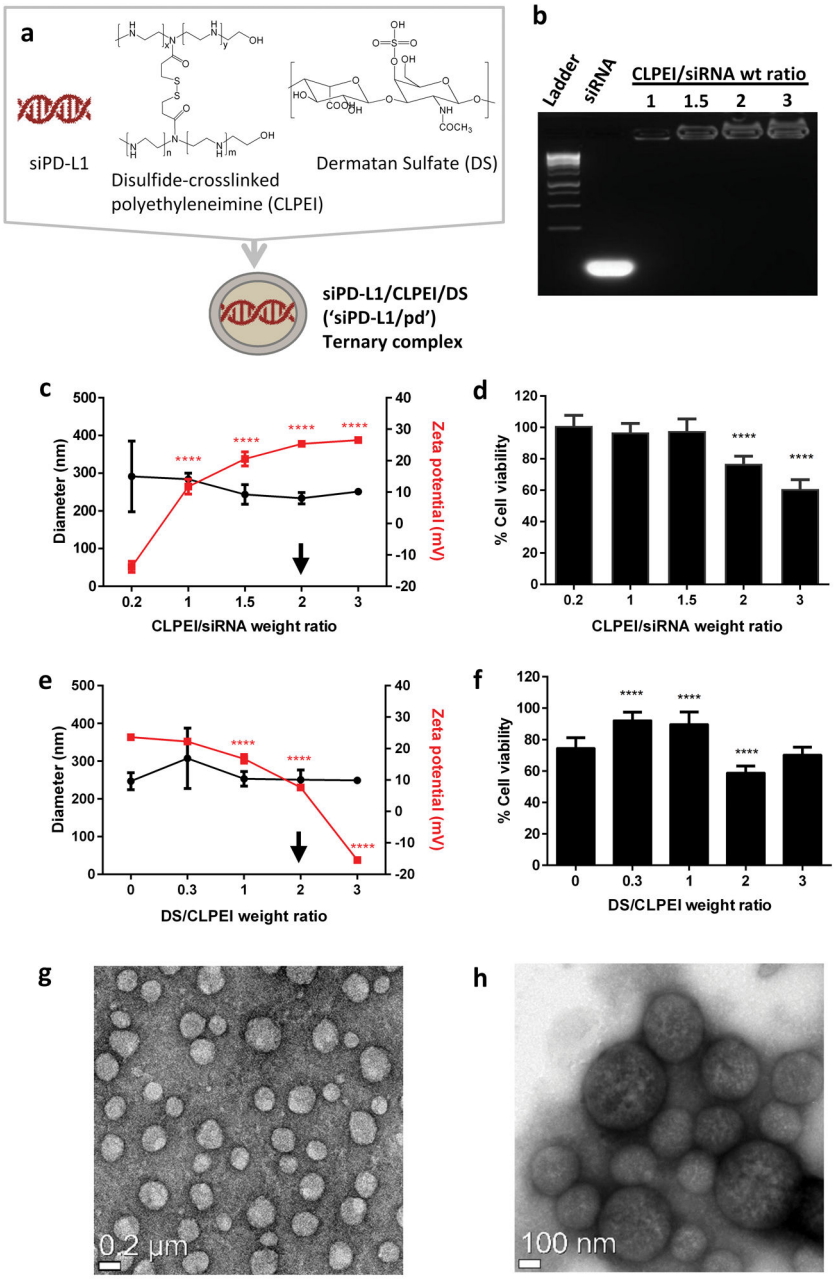

Figure 1.

(a) Schematic of siPD-L1/CLPEI/DS ('siPD-L1/pd') ternary complex. (b) Formation of siRNA-CLPEI binary complexes, confirmed by electrophoresis. (c) Hydrodynamic diameters (circle) and zeta potentials (square) of siRNA-CLPEI binary complexes with different CLPEI/siRNA ratios. n = 3 identically prepared samples, mean ± s.d. (d) Viability of B16F10 cells after 6 h incubation with binary complexes and additional incubation for 42 h in treatment-free medium. n = 3 identically prepared samples, mean ± s.d. ****: $p < 0.0001$ vs. CLPEI/siRNA ratio of 0.2 by Dunnett's test. (e) Hydrodynamic diameters (circle) and zeta potentials (square) of siRNA-CLPEI-DS ternary complexes with different DS/CLPEI ratios (CLPEI/siRNA ratio fixed at 2). n = 3 identically prepared samples, mean ±

s.d. (f) Viability of B16F10 cells after 6 h incubation with ternary complexes and additional incubation for 42 h in treatment-free medium. n = 3 identically prepared samples, mean ± s.d. ****: $p < 0.0001$ vs. DS/CLPEI ratio of 0 by Dunnett's test. (g–h) TEM images of siPD-L1/pd complex. Low magnification (g) and high magnification (h).

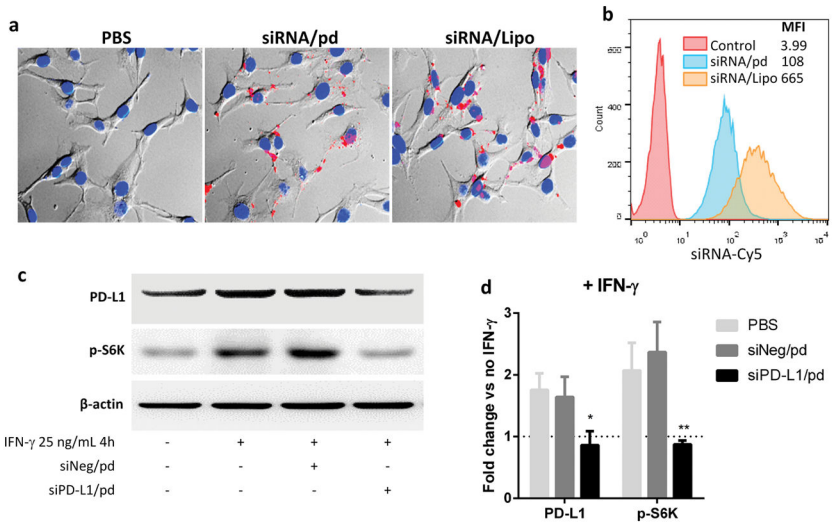

Figure 2.

Uptake of siRNA/pd complex by B16F10 melanoma cells observed with (a) fluorescence microscopy (red: Cy 5-labeled siRNA; blue: nuclei) and (b) flow cytometry. (c) Representative western blotting image demonstrating the silencing of PD-L1 and p-S6K expression in IFN-γ–activated B16F10 cells by siPD-L1/pd complex. (d) Quantitative presentation of western blotting. n = 3 separate experiments, mean ± s.d. *: $p < 0.05$, **: $p < 0.01$ *vs.* PBS group by Sidak's multiple comparisons test.

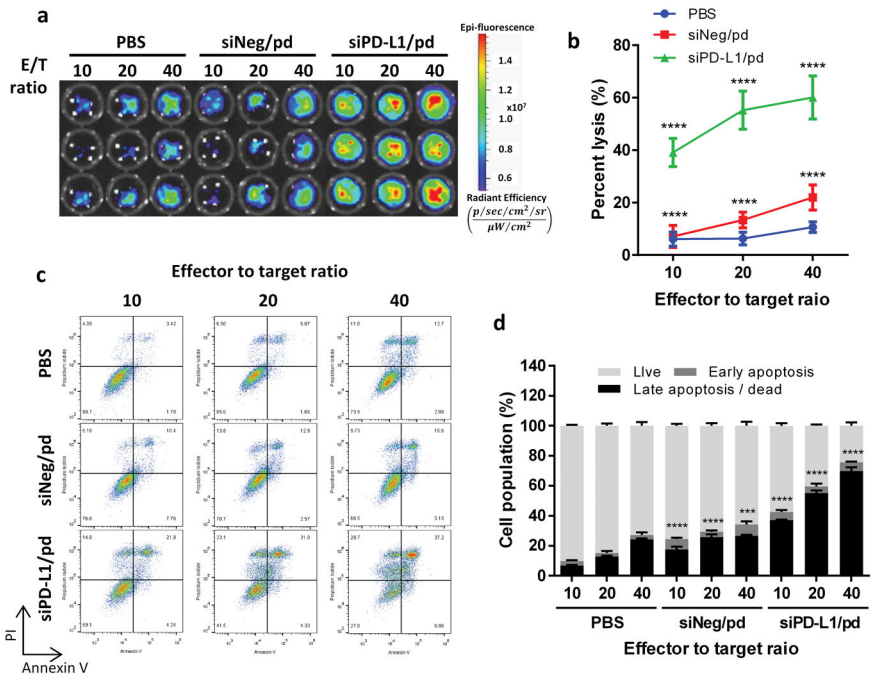

Figure 3.

In vitro cytolytic activity of OT-1 splenocytes (effector cells) and apoptosis of B16F10-OVA cells (target cells). (a) Deep red fluorescence of B16F10-OVA cell lysates. (b) Region of interest (ROI) fluorescence intensity of B16F10-OVA cell lysates. n = 3 replicates in a representative experiment, mean ± s.d. ****: $p < 0.0001$ *vs.* PBS group by Dunnett's multiple comparisons test. (c) Representative dot plots showing B16F10 cells undergoing apoptosis and necrosis, stained with Annexin V-PI. (d) Percentages of cell population undergoing apoptosis and death determined by dual-color analysis. n = 3 replicates in a representative experiment. ***: $p < 0.001$ and ****: $p < 0.0001$ *vs.* PBS in Σ(apoptotic or dead cells) at each effector to target ratio by Dunnett's multiple comparisons test.

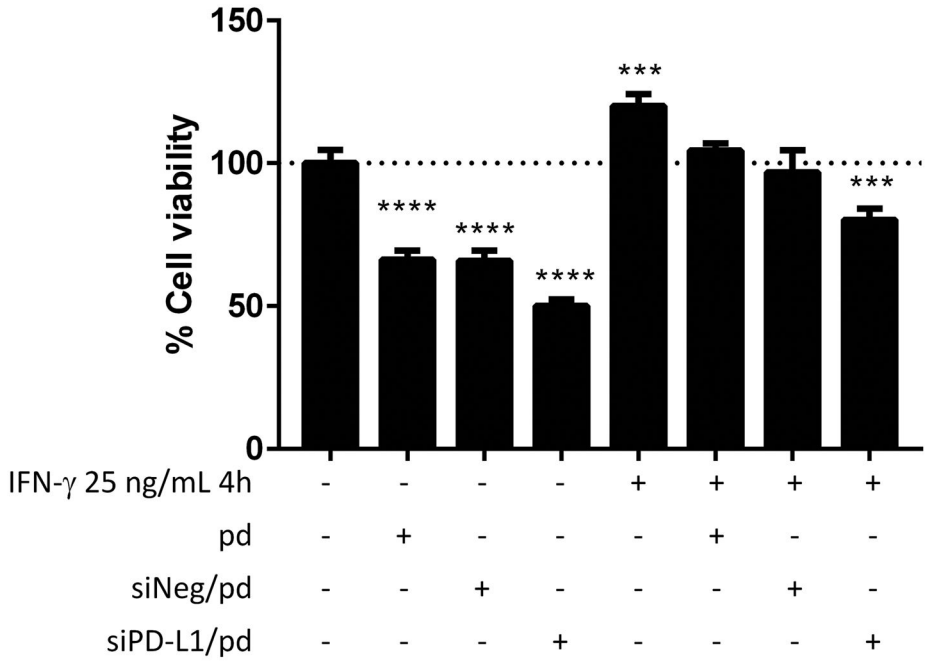

Figure 4.

Viability of B16F10 cells treated with IFN-γ, pd and siRNA/pd. n = 3 replicates in a representative experiment, mean ± s.d. ***: $p < 0.001$, ****: $p < 0.0001$ *vs.* PBS-treated group by Dunnett's multiple comparisons test.

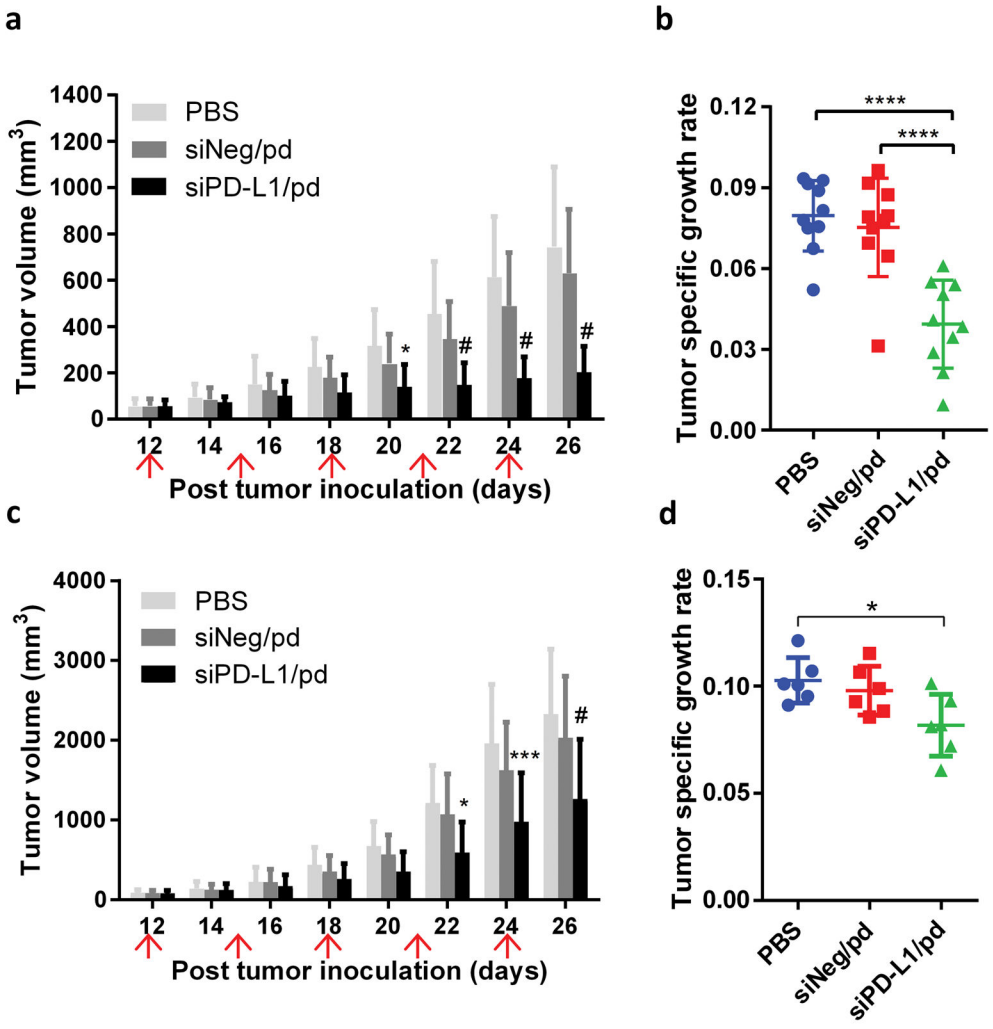

Figure 5.

B16F10 subcutaneous tumor growth in (a, b) immune-competent C57BL/6 (n = 10 per group) and (c, d) immune-compromised Balb/c nude mice (n = 6 per group). 1.5 mg siRNA per kg, q3d × 5. mean ± s.d. (a) Tumor volume change in C57BL/6 mice. *: $p < 0.05$; #: $p < 0.0001$ *vs.* PBS group at each day by Dunnett's test. (b) Tumor specific growth rate in C57BL/6 mice. ****: $p < 0.0001$ by Tukey's multiple comparisons test. (c) Tumor volume change in Balb/c nude mice. *: $p < 0.05$; ***: $p < 0.001$; #: $p < 0.0001$ *vs.* PBS group at each day by Dunnett's test. (d) Tumor specific growth rate in Balb/c nude mice. *: $p < 0.05$ by Tukey's multiple comparisons test.

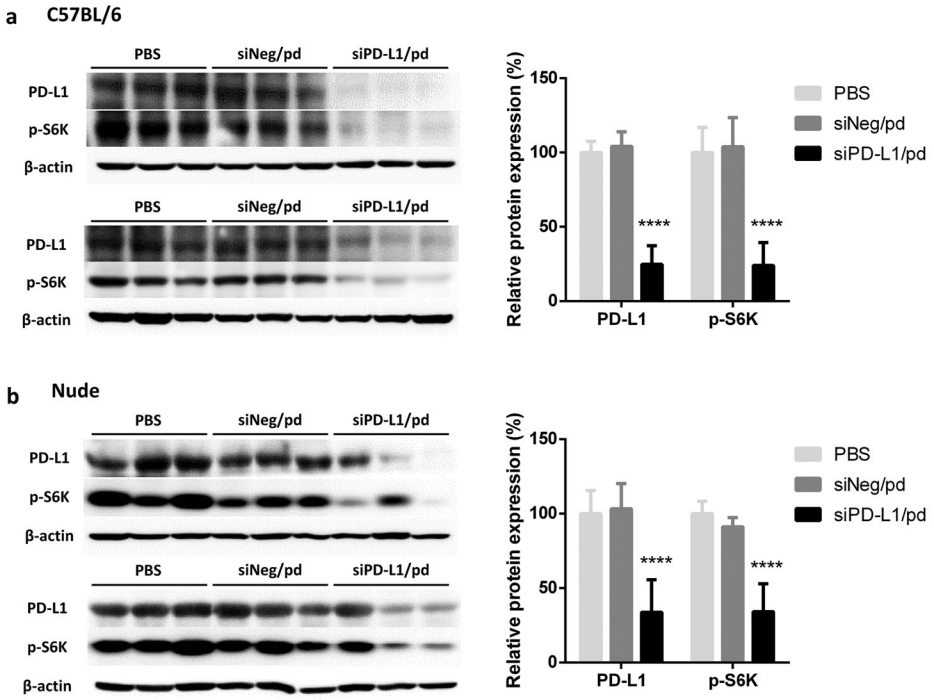

Figure 6.

Expression of PD-L1 and p-S6K in tumors in (a) C57BL/6 and (b) Balb/c nude mice. n = 6 mice per group, mean ± s.d. ****: $p < 0.0001$ *vs.* other groups by Tukey's multiple comparisons test.

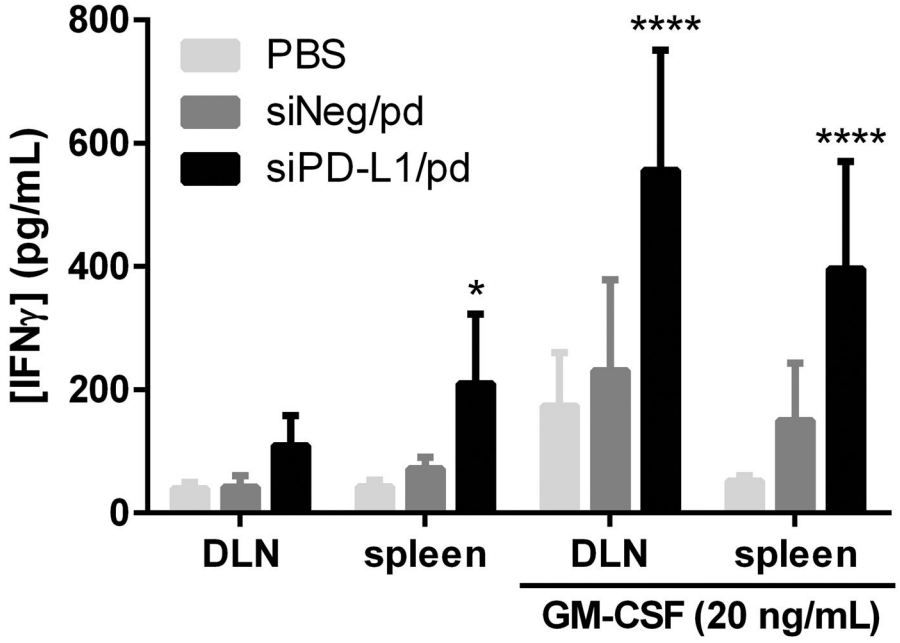

Figure 7.

IFN-γ secretion from DLN cells and splenocytes of C57BL/6 mice receiving different treatments. n = 6 mice per group, mean ± s.d. *: $p < 0.05$, ****: $p < 0.0001$ *vs.* PBS group by Dunnett's multiple comparisons test.

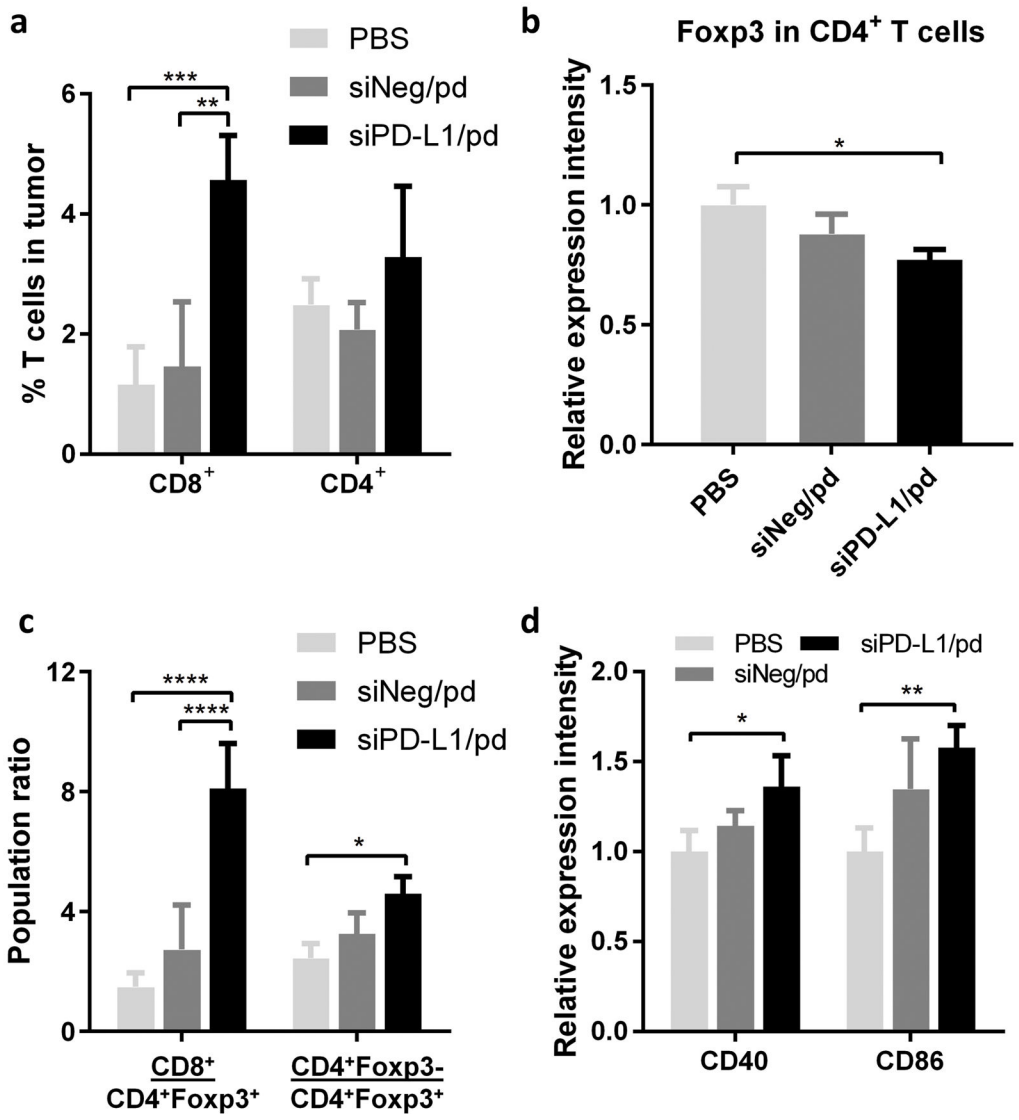

Figure 8.

(a) % $CD8^+$ and $CD4^+$ T cells in B16F10-OVA tumors of C57BL/6 mice receiving different treatments (also see Figure S6 and 7). (b) Relative intensity of Foxp3 expression on $CD4^+$ T cells in B16F10-OVA tumors (also see Figure S7). (c) Ratios of $CD8^+$ T cells to $CD4^+Foxp3^+$ T cells and $CD4^+Foxp3^-$ T cells to $CD4^+Foxp3^+$ T cells in B16F10-OVA tumors. (d) Relative expression intensity of DC maturation markers (CD40, CD86) on DCs in DLNs of C57BL/6 mice with B16F10-OVA tumors receiving different treatments (also see Figure S8). n =3 mice per group, mean ± s.d. *: $p<0.05$; **: $p < 0.01$; ***: $p < 0.001$; ****: $p < 0.0001$ by Tukey's multiple comparisons test.

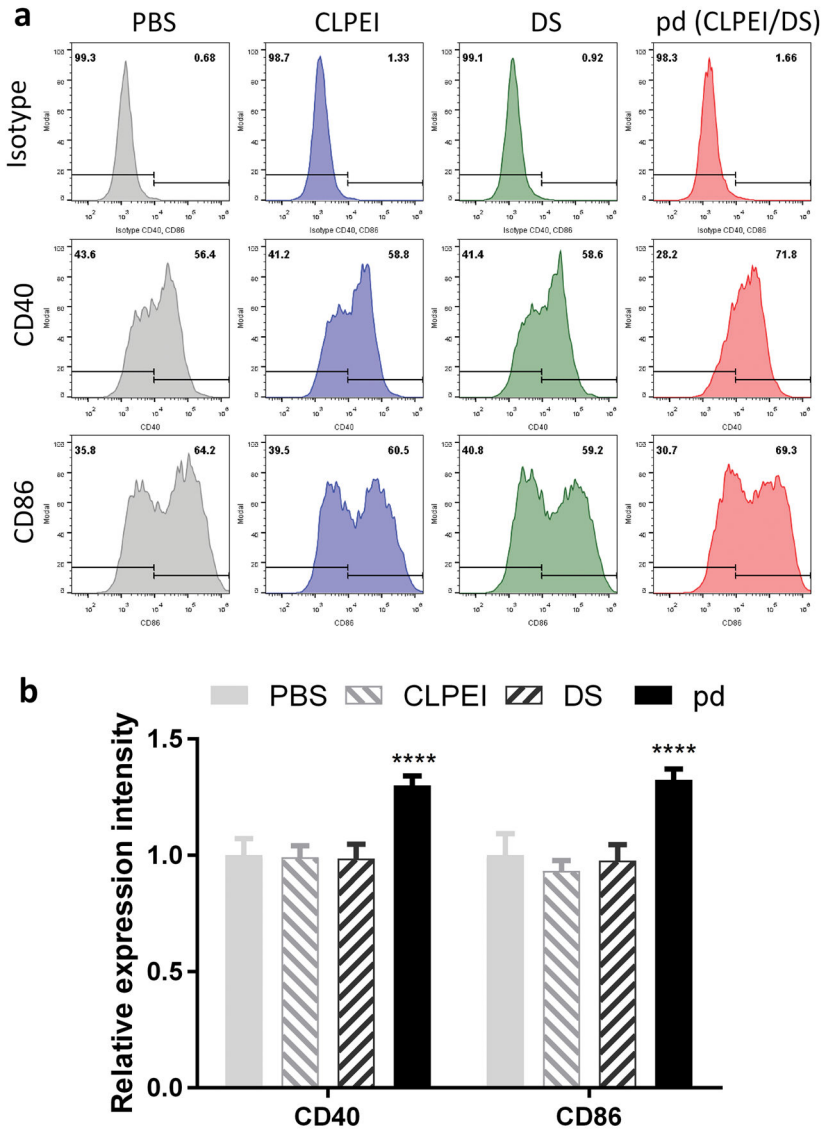

Figure 9.

(a) Expression of CD40 and CD86 on $CD11^{c+}$ BMDCs treated with PBS, CLPEI (3 μg/mL), DS (6 μg/mL), or pd (CLPEI:DS = 1:2, eq. to 3 μg/mL CLPEI). (b) Relative expression intensity of CD40 and CD86. n = 3 separate experiments, mean ± s.d. ****: $p < 0.0001$ vs. PBS-treated BMDCs by Dunnett's multiple comparisons test (also see Figure S9).